

# Pd-containing perovskite-type oxides used for three-way catalysts

Kebin Zhou\*, Hongde Chen, Qun Tian, Zhengping Hao, Dixin Shen, Xiaobai Xu

*Research Center for Eco-Environmental Sciences, Chinese Academy of Sciences, Beijing 100085, China*

Received 24 October 2001; received in revised form 24 January 2002; accepted 11 March 2002

## Abstract

Two types of catalysts with the same palladium loading, palladium-substituted perovskite ( $\text{LaFe}_{0.77}\text{Co}_{0.17}\text{Pd}_{0.06}\text{O}_3$ ) and perovskite-supported palladium catalyst ( $\text{Pd/LaFe}_{0.8}\text{Co}_{0.2}\text{O}_3$ ) were prepared, and the effects of the preparation methods and reactant gas composition on the catalytic behaviors were investigated in detail. The catalyst structure was characterized by X-ray diffraction (XRD), transmission electron micrograph (TEM), temperature-programmed reduction (TPR) and X-ray photoelectron spectroscopy (XPS) techniques. It was found that the excellent three-way catalytic activities could be obtained under slight rich conditions due to hydrocarbon steam reforming. The activity performance of  $\text{Pd/LaFe}_{0.8}\text{Co}_{0.2}\text{O}_3$  was higher than that of  $\text{LaFe}_{0.77}\text{Co}_{0.17}\text{Pd}_{0.06}\text{O}_3$  and this was owing to the ease of reduction of palladium in the former.

© 2002 Elsevier Science B.V. All rights reserved.

*Keywords:* Palladium-substituted; Supported; Perovskite-type oxide; Three-way catalyst; Light-off

## 1. Introduction

The typical three-way catalyst (TWC) formulations are those containing both platinum (Pt) and rhodium (Rh). The Rh/Pt ratio in TWC with sufficient durability is considerably higher than mine ratio [1]. Palladium is well known to have a better resistance to thermal sintering, lower price than Pt and Rh, and also have a good activity for the oxidation of hydrocarbon and carbon monoxide [2–5]. Recent attention has been concentrated on the use of palladium-based catalyst for TWC formulations.

The chemical state of palladium is a critical parameter for a good activity [6]. Generally, the chemical state and the activity of supported Pd catalysts have been reported to depend on the type of metal oxide support and the preparation processes [7]. However,

most of these Pd catalysts are supported on simple metal oxides, such as  $\text{Al}_2\text{O}_3$ ,  $\text{TiO}_2$ , and  $\text{ZrO}_2$ . Using perovskite-type oxides as support materials was relatively seldom.

In recent years, perovskites have been investigated extensively in catalysis, and have been also proposed as potential TWC instead of classical Pt/Rh-based catalysts [8]. Since the catalytic property of perovskite-type oxides is greatly depended on the nature of B-site cations [9], the selection of B-site cations is of importance in designing perovskites as well as in improving their catalytic properties. The most frequently used B-site cations are Co and Fe because they are very active for oxidation reactions. Recently, the partial substitution at B-sites of perovskites with the cations of Co and Fe has proven to be very effective in promoting catalytic activity [10–12].

Combining noble metals with perovskites can stabilize the metal against sintering, reaction with the support, or volatilization. It can also enhance the activity

\* Corresponding author. Tel.: +86-10-6284-9119;  
fax: +86-10-6292-3563.  
E-mail address: kbzhou@hotmail.com (K. Zhou).

of simple perovskite when small amounts of a noble metal are added [12–14]. Guilhaume et al. [13] reported that the activity of palladium-substituted lanthanum cuprates,  $\text{La}_2\text{Cu}_{0.8}\text{Pd}_{0.2}\text{O}_4$ , was comparable to that of Pt–Rh/CeO<sub>2</sub>–Al<sub>2</sub>O<sub>3</sub> catalyst for NO reduction, and higher for CO and C<sub>3</sub>H<sub>6</sub> oxidation. Also Tanaka et al. [12] reported that perovskite-supported palladium (Pd/(LaCe)(CoFe)O<sub>3</sub>) had excellent potentiality for automotive exhaust purification as non-rhodium catalysts. It should be noticed that palladium was on the surface of the perovskite in this case, while the noble metal was at the B-site in the palladium-substituted perovskite. It can be reasonable that the chemical state and the redox behavior of palladium would be different between the palladium-substituted perovskite and the perovskite-supported catalysts. However, relatively little was reported.

In this work,  $\text{LaFe}_{0.8}\text{Co}_{0.2}\text{O}_3$  was chosen as the support material; two kinds of catalyst, palladium-substituted perovskite ( $\text{LaFe}_{0.77}\text{Co}_{0.17}\text{Pd}_{0.06}\text{O}_3$ ) and perovskite-supported palladium ( $\text{Pd/LaFe}_{0.8}\text{Co}_{0.2}\text{O}_3$ ) were prepared and measured under a condition approaching the real working cases of TWC.

## 2. Experimental

### 2.1. Catalysts preparation

$\text{LaFe}_{0.77}\text{Co}_{0.17}\text{Pd}_{0.06}\text{O}_3$  was prepared by using a conventional coprecipitation method. In the synthesis process,  $\text{La}(\text{NO}_3)_3 \cdot 6\text{H}_2\text{O}$ ,  $\text{Co}(\text{NO}_3)_2 \cdot 6\text{H}_2\text{O}$ ,  $\text{Fe}(\text{NO}_3)_3 \cdot 9\text{H}_2\text{O}$ ,  $\text{PdCl}_2$  and  $\text{NH}_4\text{HCO}_3 \cdot \text{H}_2\text{NCOONH}_4$  (all in AR grade purity) were used. A solution of the metal nitrates of appropriate La, Fe, Co and Pd concentrations was prepared and then added to a solution of ammonium carbonate. The precipitate was washed, dried at 120 °C for 24 h, calcined in air at 900 °C for 5 h, and then the powdered  $\text{LaFe}_{0.77}\text{Co}_{0.17}\text{Pd}_{0.06}\text{O}_3$  samples was obtained.

$\text{Pd/LaFe}_{0.8}\text{Co}_{0.2}\text{O}_3$  was prepared by impregnating a  $\text{LaFe}_{0.8}\text{Co}_{0.2}\text{O}_3$  carrier (prepared by coprecipitation method as stated above) with an aqueous solution containing a desired amount of  $\text{PdCl}_2$  (AR grade). After drying at 120 °C, the catalyst was calcined at 600 °C for 5 h in air.  $\text{LaFe}_{0.77}\text{Co}_{0.17}\text{Pd}_{0.06}\text{O}_3$  and  $\text{Pd/LaFe}_{0.8}\text{Co}_{0.2}\text{O}_3$  were prepared with the same palladium loading, ca. 2.6 wt.%. All catalyst samples

were pressed and sieved to a size of 10–20 meshes for the activity evaluation.

### 2.2. Catalytic activity evaluation

The activity measurements were carried out in a fixed-bed quartz tubular reactor at atmospheric pressure. Catalyst particles (4 ml) were placed in the reactor. Inlet temperature was measured at the place of 2 mm from the front side of the catalyst bed. The temperature inside the reactor was increased continuously from 100 to 500 °C at a rate of 5 °C min<sup>-1</sup>, while the reactant gases went through the reactor with a space velocity of 45,000 h<sup>-1</sup>. Analysis of the effluent gas was performed on an AVL DiGas 4000 detector.

The experimental feed stream simulated the actual automotive exhaust gas composition under rich or stoichiometric condition. The stoichiometric number, *S*, was used as a redox characteristic of the feed stream:  $S = (2[\text{O}_2] + [\text{NO}]) / ([\text{CO}] + 9[\text{C}_3\text{H}_6] + 10[\text{C}_3\text{H}_8])$ . All concentrations are expressed in vol.%. The light-off performance of each catalyst was studied in either a rich (1.8 vol.% CO, 10 vol.% CO<sub>2</sub>, 0.08 vol.% NO, 0.2 vol.% HC (C<sub>3</sub>H<sub>6</sub>:C<sub>3</sub>H<sub>8</sub> = 1:1), 1.63 vol.% O<sub>2</sub>, balanced with nitrogen, *S* = 0.9) or a stoichiometric (1.8 vol.% CO, 10 vol.% CO<sub>2</sub>, 0.08 vol.% NO, 0.2 vol.% HC (C<sub>3</sub>H<sub>6</sub>:C<sub>3</sub>H<sub>8</sub> = 1:1), 1.81 vol.% O<sub>2</sub>, balanced with nitrogen, *S* = 1.0) reactant gas mixture. The conversions of CO, HC and NO were measured and recorded as functions of the inlet temperature.

### 2.3. Catalysts characterization

BET-surface area of catalysts was measured by N<sub>2</sub> adsorption using the single point method. The BET areas were 8.3 and 9.0 m<sup>2</sup> g<sup>-1</sup> for  $\text{LaFe}_{0.77}\text{Co}_{0.17}\text{Pd}_{0.06}\text{O}_3$  and  $\text{Pd/LaFe}_{0.8}\text{Co}_{0.2}\text{O}_3$ , respectively. X-ray diffraction (XRD) measurements were carried out on a Rigaku D/MAX-RB diffractometer with Cu K $\alpha$  radiation. TEM measurements were performed by a JEM 200CX transmission electron microscope. XPS measurements were conducted on a VG ESCA LAB 220 i-XL system with Al K $\alpha$  radiation under UHV ( $5 \times 10^{-9}$  Pa), calibrated internally by carbon deposit C (1s) binding energy (BE) at 284.6 eV. In order to understand the nature of the catalyst surface, XPS analysis was performed over fresh (pre-reaction)

and post-reaction (in rich ( $S = 0.9$ ) reactant gas compositions) catalysts, respectively.

Hydrogen temperature-programmed reduction ( $H_2$ -TPR) of catalyst was conducted on a fixed-bed continuous flow reactor connected with GC combination system. The catalyst sample (60 mg) was flushed by a purified nitrogen stream, first at  $400\text{ }^\circ\text{C}$  for 30 min and then cooled down to room temperature, followed by flushing with a nitrogen-carrying 5 vol.%  $H_2$  gaseous mixture as a reducing gas for starting TPR test. The temperature increased at a rate of  $10\text{ }^\circ\text{C min}^{-1}$ . Change of hydrogen signal was monitored using an on-line GC with a thermal conductivity detector (TCD).

### 3. Results and discussion

#### 3.1. Catalytic activity

##### 3.1.1. Light-off catalytic performance in a stoichiometric ( $S = 1$ ) reactant gases

The light-off performance of the two catalysts,  $LaFe_{0.77}Co_{0.17}Pd_{0.06}O_3$  and  $Pd/LaFe_{0.8}Co_{0.2}O_3$ , were tested in a stoichiometric ( $S = 1$ ) reactant gas mixture. Table 1 summarizes the light-off temperatures  $T_{50}$  and  $T_{90}$ , corresponding to 50 and 90% conversion of the pollutants.

As seen in Fig. 1 and Table 1, in the case of palladium-substituted perovskite ( $LaFe_{0.77}Co_{0.17}Pd_{0.06}O_3$ ), the conversion of the three pollutants started at about  $225\text{ }^\circ\text{C}$ , and the  $T_{90}$  for CO, HC and NO were at 238, 416 and  $433\text{ }^\circ\text{C}$ , respectively. For the  $Pd/LaFe_{0.8}Co_{0.2}O_3$  catalyst, the conversions of CO and NO started at about  $180\text{ }^\circ\text{C}$  and the conversion of hydrocarbon at about  $200\text{ }^\circ\text{C}$ . The  $T_{90}$  for CO, HC and NO were at 208, 242 and  $267\text{ }^\circ\text{C}$ , respectively.

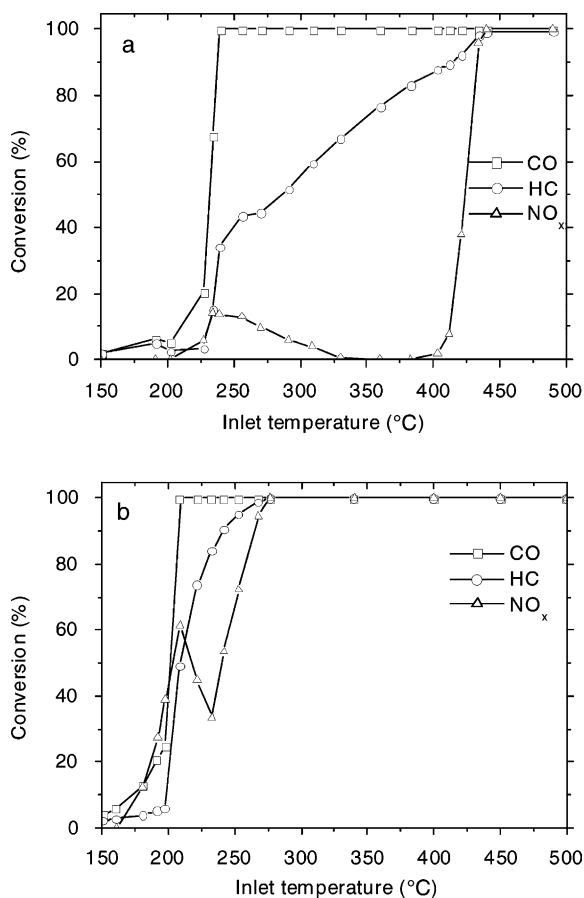


Fig. 1. Light-off performance in stoichiometric ( $S = 1.0$ ) reactant gas over catalyst: (a)  $LaFe_{0.77}Co_{0.17}Pd_{0.06}O_3$  and (b)  $Pd/LaFe_{0.8}Co_{0.2}O_3$ .

The reaction data show that the preparation methods have a great impact on the catalytic activities. In general, the perovskite-supported palladium ( $Pd/LaFe_{0.8}Co_{0.2}O_3$ ) catalyst appeared to be much active than

Table 1

Conversion data expressed as  $T_{50}$  and  $T_{90}$  ( $^\circ\text{C}$ ) of  $Pd/LaFe_{0.8}Co_{0.2}O_3$  and  $LaFe_{0.77}Co_{0.17}Pd_{0.06}O_3$  under rich ( $S = 0.9$ ) and stoichiometric ( $S = 1.0$ ) steady-state conditions

Stoichiometric number ( $S$ )	Catalyst	CO		HC		NO	
		$T_{50}$	$T_{90}$	$T_{50}$	$T_{90}$	$T_{50}$	$T_{90}$
1.0	$LaFe_{0.77}Co_{0.17}Pd_{0.06}O_3$	233	238	290	416	425	433
	$Pd/LaFe_{0.8}Co_{0.2}O_3$	204	208	209	242	241	267
0.9	$LaFe_{0.77}Co_{0.17}Pd_{0.06}O_3$	241	243	301	347	342	348
	$Pd/LaFe_{0.8}Co_{0.2}O_3$	214	216	213	216	210	215

the palladium-substituted perovskite ( $\text{LaFe}_{0.77}\text{Co}_{0.17}\text{Pd}_{0.06}\text{O}_3$ ).

### 3.1.2. Influence of reactant gas composition on the light-off performance

When the catalysts were subjected to a rich ( $S = 0.9$ ) reactant gas compositions, as expected,  $T_{50}$  and  $T_{90}$  for CO and  $T_{50}$  for HC conversion were increased, and the catalytic performance for NO seemed to be improved remarkably (shown in Table 1 and Fig. 2(a) and (b)). Although the overall conversion of CO is only 93%, the activities of HC and NO are much higher as compared to that under stoichiometric conditions ( $S = 1$ ).

It should be pointed out that  $T_{90}$  for HC was decreased and the light-off temperature ‘window’ of HC

became narrower for both the two catalysts. Product analysis showed that there was a small amount of hydrogen in the reactor exhaust when oxygen was totally consumed under rich condition ( $S = 0.9$ ). It indicates that hydrocarbon steam reforming (SR) might occur (Eq. (1))



The water comes from the hydrocarbon oxidation. Maillot et al. [6] also observed a secondary SR reaction over a  $\text{Pd}/\text{Al}_2\text{O}_3$  catalyst. Then the promoted HC conversion under rich condition could be attributed to the SR. Further, CO appears to be more reactive than hydrocarbons from the data. However, the oxidation of CO rather than the oxidation of hydrocarbon is left incomplete under rich condition. The explanation is also the SR: hydrogen, produced by the SR reaction, is easier to be oxidized (by NO or  $\text{O}_2$ ) than CO.

It can be seen from Figs. 1 and 2 that the NO conversion increased with increasing temperature until at a certain reaction temperature, and then decreased with further increase to 100%. Martínez-Arias et al. [15] believed that conversion of NO at lower temperatures corresponded to adsorption/desorption processes, as calculated from mass balance of the outlet gases. It is obvious that the conversion of NO is always complete after overall oxidation of HC. This is mostly because that there was some amount of oxygen left in the reactant gas mixture before complete conversion of reducing reactants (CO and HC) [16].

## 3.2. Catalyst characterizations

### 3.2.1. XRD patterns

The crystal compositions of the catalysts were determined by XRD and the patterns of the catalysts are presented in Fig. 3. The XRD pattern of  $\text{LaFe}_{0.8}\text{Co}_{0.2}\text{O}_3$  shows that purely perovskite crystallinity could be obtained after calcinations at  $900^\circ\text{C}$ . The palladium-substituted perovskite ( $\text{LaFe}_{0.77}\text{Co}_{0.17}\text{Pd}_{0.06}\text{O}_3$ ) is also a single-phase perovskite-type oxide, which shows sharp and well-defined superstructure reflections. No lines corresponding to palladium oxide or metal can be observed. Moreover, the XRD line shows a small shift to higher  $2\theta$  values with respect to  $\text{LaFe}_{0.8}\text{Co}_{0.2}\text{O}_3$ . It indicates that palladium is incorporated into the perovskite structure and the crystallinity tends to be changed. Addition to

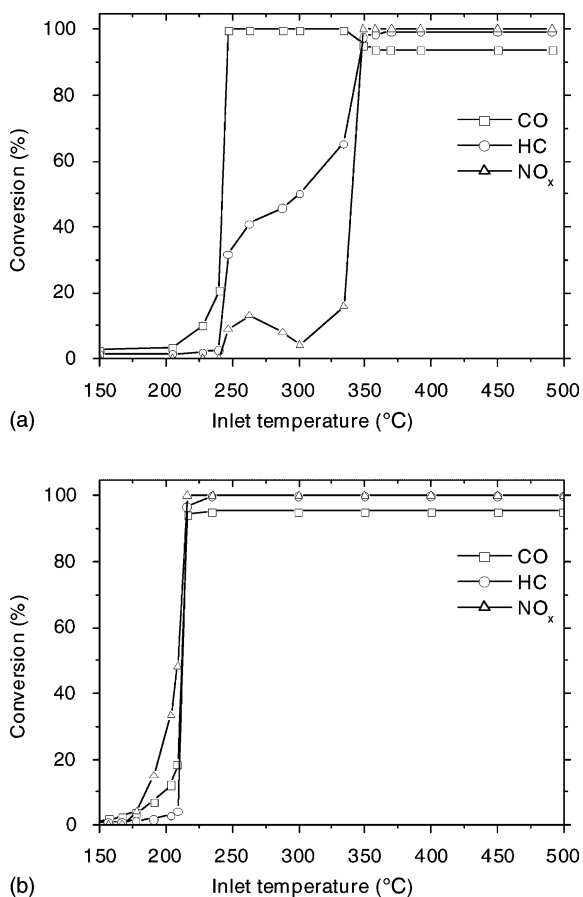


Fig. 2. Light-off performance in rich ( $S = 0.9$ ) reactant gas over catalyst: (a)  $\text{LaFe}_{0.77}\text{Co}_{0.17}\text{Pd}_{0.06}\text{O}_3$  and (b)  $\text{Pd}/\text{LaFe}_{0.8}\text{Co}_{0.2}\text{O}_3$ .

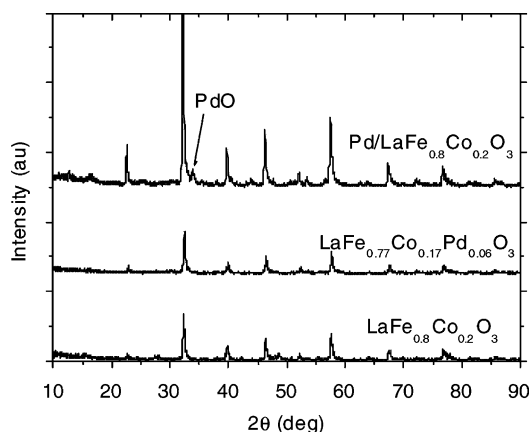


Fig. 3. XRD analysis of the solids:  $\text{LaFe}_{0.8}\text{Co}_{0.2}\text{O}_3$ ,  $\text{LaFe}_{0.77}\text{Co}_{0.17}\text{Pd}_{0.06}\text{O}_3$  and  $\text{Pd/LaFe}_{0.8}\text{Co}_{0.2}\text{O}_3$ .

perovskite phase, the pattern of  $\text{Pd/LaFe}_{0.8}\text{Co}_{0.2}\text{O}_3$  also shows a small peak at ca. 33 ( $2\theta$  value) which can be assigned to PdO [17]. No additional lines can be found in the XRD patterns.

### 3.2.2. Transmission electron micrograph (TEM)

Fig. 4 shows the TEM images of  $\text{LaFe}_{0.77}\text{Co}_{0.17}\text{Pd}_{0.06}\text{O}_3$  and  $\text{Pd/LaFe}_{0.8}\text{Co}_{0.2}\text{O}_3$  samples after activity evaluation. It can be observed that the perovskite particles distributed between 50 and 200 nm, and most of them are located at around 100 nm.

There was no Pd particles could be discerned from the surface of  $\text{LaFe}_{0.77}\text{Co}_{0.17}\text{Pd}_{0.06}\text{O}_3$ . However, a relatively homogeneous distribution of palladium particles (ca. 10 nm) is obtained over  $\text{Pd/LaFe}_{0.8}\text{Co}_{0.2}\text{O}_3$  catalyst. The Pd particles are mostly fixed on the well-developed planes of the crystalline  $\text{LaFe}_{0.8}\text{Co}_{0.2}\text{O}_3$ . Except for some Pd particles with the shape of spherical and weakly attached over the surface of the support, most of the Pd particles are hemispherical in shape, and the interface between Pd and  $\text{LaFe}_{0.8}\text{Co}_{0.2}\text{O}_3$  can be clearly observed. Consequently, such matching of the structure could stabilize Pd particles and favor a strong metal–support interaction.

XRD and TEM results show that most of palladium exists on the surface of the catalyst over  $\text{Pd/LaFe}_{0.8}\text{Co}_{0.2}\text{O}_3$ , while it is in the crystalline of the palladium-substituted perovskite,  $\text{LaFe}_{0.77}\text{Co}_{0.17}\text{Pd}_{0.06}\text{O}_3$ .

### 3.2.3. TPR

In order to explore the reason for the differences in the observed catalytic activity of these two catalysts, TPR experiments were carried out. For comparison, hydrogen TPR over  $\text{LaFe}_{0.8}\text{Co}_{0.2}\text{O}_3$  was also performed.

It can be seen from Fig. 5 that a strong peak appears at about 550 °C over  $\text{LaFe}_{0.8}\text{Co}_{0.2}\text{O}_3$ . It was reported that when  $\text{LaFeO}_3$  was subjected to TPR, no obvious peak was observed until 900 °C [18]. Hence, this increase in the reducibility of  $\text{LaFe}_{0.8}\text{Co}_{0.2}\text{O}_3$  can be attributed to the presence of cobalt at B-sites of perovskite. Wu et al. [19] reported that doping with cobalt ions in B-site of  $\text{LaFeO}_3$  could modify the redox property and reduction temperature and the reduction peak of  $\text{LaFe}_{0.8}\text{Co}_{0.2}\text{O}_3$  can be ascribed to  $\text{Fe}^{4+} \rightarrow \text{Fe}^{3+}$ .

The reduction temperature, the reduction rate, the shape and the number of peaks were changed after palladium was added. Large peaks still appear in the 420–600 °C region, and this can be assigned to the reduction of  $\text{Fe}^{4+}$  to  $\text{Fe}^{3+}$  according to the above discussion. However, the temperature of maximum uptake of hydrogen ( $T_{\text{max}}$ ) shifts down. It suggests that the reducibility of the perovskites was increased after Pd was added. It is reported that hydrogen can dissociate at the surface of the palladium and successively spillover to the support [7]. Then spillover of hydrogen may account for the lower reduction temperature.

Additionally, new peaks appear in the lower temperature region. The  $T_{\text{max}}$  are 85 and 240 °C, for  $\text{Pd/LaFe}_{0.8}\text{Co}_{0.2}\text{O}_3$  and  $\text{LaFe}_{0.77}\text{Co}_{0.17}\text{Pd}_{0.06}\text{O}_3$ , respectively. These peaks probably correspond to the reduction of palladium (II),  $\text{Pd}^{2+} \rightarrow \text{Pd}^0$  [7,20]. For  $\text{Pd/LaFe}_{0.8}\text{Co}_{0.2}\text{O}_3$  catalyst, the reduction temperature is 85 °C, which is much lower than that over  $\text{LaFe}_{0.77}\text{Co}_{0.17}\text{Pd}_{0.06}\text{O}_3$  catalyst ( $T_{\text{max}} = 240$  °C). Another peak can also be seen at higher temperature region (600–700 °C) over  $\text{LaFe}_{0.77}\text{Co}_{0.17}\text{Pd}_{0.06}\text{O}_3$ , while there is no  $\text{H}_2$  consumption peak in  $\text{Pd/LaFe}_{0.8}\text{Co}_{0.2}\text{O}_3$  catalyst. This indicates palladium introduced by coprecipitation occupy B-sites of the perovskite and affect the properties of crystal oxygen in  $\text{ABO}_3$  structure.

### 3.2.4. XPS spectra

XPS studies of the catalysts were performed pre- and post-reaction in rich reactant gas compositions ( $S = 0.9$ ). Fig. 6(a) shows the XPS spectra of Pd 3d

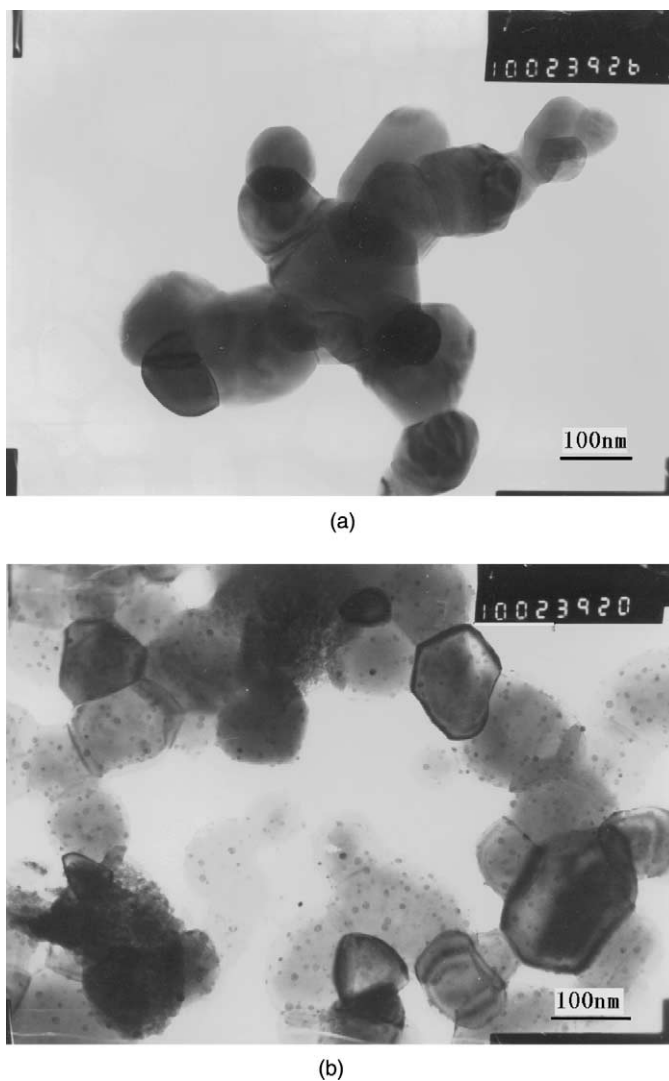


Fig. 4. TEM photographs of catalysts: (a)  $\text{LaFe}_{0.77}\text{Co}_{0.17}\text{Pd}_{0.06}\text{O}_3$  and (b)  $\text{Pd/LaFe}_{0.8}\text{Co}_{0.2}\text{O}_3$ .

core level of fresh samples. The peaks of the Pd 3d over  $\text{Pd/LaFe}_{0.8}\text{Co}_{0.2}\text{O}_3$  appeared at 336.7 eV, which is assigned to palladium (II) oxide [21,22]. While there was almost no signal could be discerned from the surface of  $\text{LaFe}_{0.77}\text{Co}_{0.17}\text{Pd}_{0.06}\text{O}_3$ . This indicates that Pd was highly dispersed in the bulk of perovskite prepared by coprecipitation.

The results of post-reaction XPS analysis for the catalysts were also listed in Fig. 6(b). Over  $\text{Pd/LaFe}_{0.8}\text{Co}_{0.2}\text{O}_3$  catalyst, the peaks of the Pd 3d

appeared at 335.2 eV with shoulder at 336.5 eV. It suggests that the most of the palladium on the surface was reduced to metallic palladium after reaction under rich conditions, whereas the rest were still in the form of  $\text{Pd}^{2+}$ . It is reported that the reduction of PdO can occur in the reactant mixture, even in an excess oxygen atmosphere [6]. Although palladium could not be detected over fresh  $\text{LaFe}_{0.77}\text{Co}_{0.17}\text{Pd}_{0.06}\text{O}_3$ , a slight  $\text{Pd}^{2+}$  signal was recorded after catalytic run. This indicates that (1) palladium was doped into the

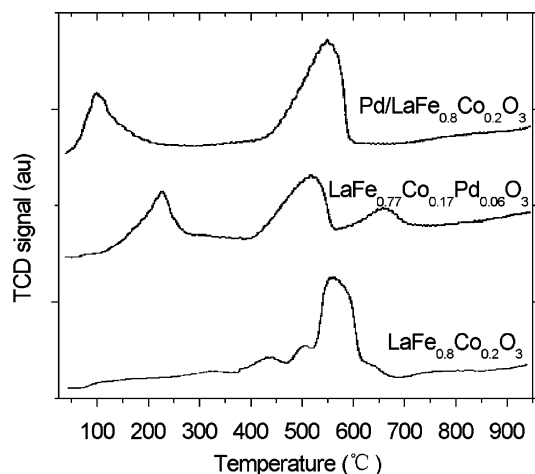
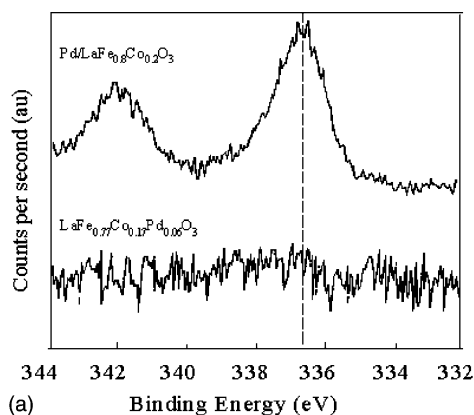
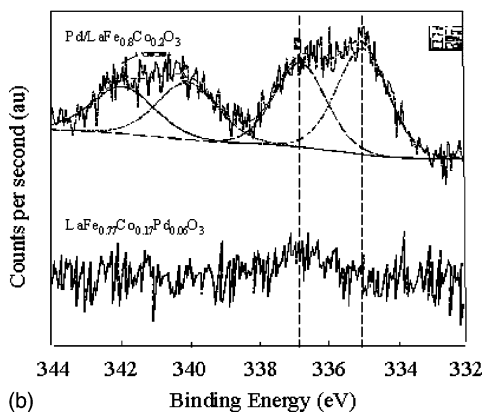


Fig. 5. TPR profiles of catalysts:  $\text{LaFe}_{0.8}\text{Co}_{0.2}\text{O}_3$ ,  $\text{Pd/LaFe}_{0.8}\text{Co}_{0.2}\text{O}_3$  and  $\text{LaFe}_{0.77}\text{Co}_{0.17}\text{Pd}_{0.06}\text{O}_3$ .



(a) Binding Energy (eV)



(b) Binding Energy (eV)

Fig. 6. XPS spectra of catalysts in the Pd 3d region: (a) pre-reaction and (b) post-reaction under rich conditions ( $S = 0.9$ ).

crystal lattice of  $\text{ABO}_3$  prepared by means of precipitation, and (2) the surface structure of perovskite-type had been modified by reactant gases during reaction.

The results of XRD, TEM and XPS show that the structures are different between the  $\text{LaFe}_{0.77}\text{Co}_{0.17}\text{Pd}_{0.06}\text{O}_3$  and the  $\text{Pd/LaFe}_{0.8}\text{Co}_{0.2}\text{O}_3$  catalyst. TPR and XPS data show that Pd added by impregnation localized on the perovskite surface and easily to be reduced, while for  $\text{LaFe}_{0.77}\text{Co}_{0.17}\text{Pd}_{0.06}\text{O}_3$ , Pd was in the lattice of perovskite-type oxide and strong interaction between Pd and O occurred and relative difficulty to be reduced. Combining with the activity results, we can conclude that the easier of the palladium to be reduced, the higher activity was obtained.

Also it should be pointed out that the support,  $\text{LaFe}_{0.8}\text{Co}_{0.2}\text{O}_3$ , is also a good catalyst itself. There is often a close relationship between the catalytic activity of perovskites and the defect density in their crystalline structure. The incorporation of Co and/or Pd into B-sites, would probably cause  $\text{ABO}_3$  exist in non-stoichiometric compositions, including typically the lattice oxygen vacancies that could form active oxygen species by adsorbing oxygen from gas phase for the oxidation reaction [8]. The oxygen vacancies are also favor for the adsorption of NO, which has the similar electron structure to oxygen. How the defects affect the properties of Pd-containing perovskites still needs further study.

#### 4. Conclusions

The following conclusions can be drawn from the results in this investigation:

- (1) The preparation methods play important roles in improving the activity of the palladium-containing perovskite catalysts. The three-way catalytic activity of perovskite-supported palladium ( $\text{Pd/LaFe}_{0.8}\text{Co}_{0.2}\text{O}_3$ ) is much higher than the palladium-substituted perovskite ( $\text{LaFe}_{0.77}\text{Co}_{0.17}\text{Pd}_{0.06}\text{O}_3$ ). Due to hydrocarbon SR, excellent three-way catalytic activities can be obtained under slight rich condition, especially for hydrocarbon oxidation and NO reduction.
- (2) The reducibility of perovskite-type oxides could be improved by addition of palladium. The  $\text{Pd/LaFe}_{0.8}\text{Co}_{0.2}\text{O}_3$  catalyst can easily be reduced than the  $\text{LaFe}_{0.77}\text{Co}_{0.17}\text{Pd}_{0.06}\text{O}_3$  catalyst. And the

higher activity of the Pd/LaFe<sub>0.8</sub>Co<sub>0.2</sub>O<sub>3</sub> catalyst is due to the ease of reduction of palladium.

## References

- [1] H. Muraki, H. Shinjoh, Y. Fujitani, *Ind. Eng. Chem. Prod. Res. Dev.* 25 (1986) 419.
- [2] D.R. Rainer, M. Koranne, S.M. Vesecky, D.W. Goodman, *J. Phys. Chem. B* 101 (1997) 10769.
- [3] J.C. Summers, W.B. Williamson, M.G. Henk, SAE Paper No. 880281, 1989.
- [4] D.D. Beck, J.W. Sommers, C.L. DiMaggio, *Appl. Catal. B* 3 (1994) 205.
- [5] R. Van Yperen, D. Linder, L. Musmann, E.S. Lox, T. Kreuzer, *Stud. Surf. Sci. Catal.* 116 (1998) 51.
- [6] T. Maillet, C. Solleau, J. Barbier Jr., D. Duprez, *Appl. Catal. B* 14 (1997) 85.
- [7] W.-J. Shen, M. Okumura, Y. Matsumura, M. Haruta, *Appl. Catal. A* 213 (2001) 225.
- [8] R.J.H. Voorhoeve, *Advanced Materials in Catalysis*, Academic Press, New York, 1977, p. 173.
- [9] N. Yamazoe, Y. Teraoka, *Catal. Today* 8 (1990) 175.
- [10] M. Weston, I.S. Metcalfe, *Solid State Ionics* 113–115 (1998) 247.
- [11] V.R. Choudhary, B.S. Uphade, S.G. Pataskar, *Fuel* 78 (1999) 919.
- [12] H. Tanaka, H. Fujikawa, I. Takahashi, SAE Paper No. 930251, 1993.
- [13] N. Guilhaume, S.D. Peter, M. Primet, *Appl. Catal. B* 10 (1996) 325.
- [14] N. Guilhaume, M. Primet, *J. Catal.* 165 (1997) 197.
- [15] A. Martínez-Arias, M. Fernández-García, A. Iglesias-Juez, A.B. Hungria, J.A. Anderson, J.C. Conesa, J. Soria, *Appl. Catal. B* 31 (2001) 51.
- [16] V.I. Pârvulescu, P. Grange, B. Delmon, *Catal. Today* 46 (1998) 233.
- [17] J. Noh, O.-B. Yang, D.H. Kim, S.I. Woo, *Catal. Today* 53 (1999) 575.
- [18] F. Martínez-Ortega, C. Batiot-Dupeyrat, G. Valderrama, J.-M. Tatibouët, C. R. Acad. Sci. Paris, Série IIc, *Chimie/Chemistry* 4 (2001) 49.
- [19] S. Liu, Z. Yu, Y. Wu, *J. Inorg. Mater.* 9 (1994) 443 (in Chinese).
- [20] J. Batista, A. Pintar, D. Mandrino, M. Jenko, V. Martin, *Appl. Catal. A* 206 (2001) 113.
- [21] D.H. Kim, S.I. Woo, O.-B. Yang, *Appl. Catal. B* 26 (2000) 285.
- [22] D.L. Mowery, M.S. Graboski, T.R. Ohno, R.L. McCormick, *Appl. Catal. B* 21 (1999) 157.